International Journal of Automotive Technology, Vol. 24, No. 2, pp. 551–558 (2023)
DOI 10.1007/s12239–023–0046–1

pISSN 1229–9138/ eISSN 1976–3832

INFLUENCE OF TIRE BELT LAYER PRESSURE SHARE RATIO ON TIRE CONTOUR AND PERFORMANCE BASED ON NEW NON-NATURAL EQUILIBRIUM CONTOUR THEORY

Chen Liang, Han Li, Jian Yang*, Guolin Wang and Lingxin Zhang

School of Automotive and Traffic Engineering, Jiangsu University, Zhenjiang 212013, China

(Received 4 April 2022; Revised 19 August 2022; Accepted 9 November 2022)

ABSTRACT–Tire contour design theory has always been studied because of its significant effect on tire performance. Based on the new non-natural equilibrium contour theory, the influence of belt pressure share ratio on the carcass contour is studied. The type of 385 / 65R22.5 all-steel radial tire was chosen as the research object and the finite element analysis technique was adopted to calculate the belt pressure share ratio. The results show that with the increase of the belt pressure share ratio, the clamping effect of belt layer on the carcass is strengthened, the curvature of tire crown in carcass contour increases and the crown curve tends to be rounded. The influence of belt pressure share ratio on wear, footprint, rolling resistance and grip performance was also explored with the finite element technology. It turned out that with the increase of the belt pressure share ratio, the tire wear increased, rolling resistance reduced, grip performance enhanced.

KEY WORDS : Radial tire, Belt pressure share ratio, Carcass contour design, Tire performance

1. INTRODUCTION

The tire carcass contour plays an important role in tire performance, therefore the design of carcass contour has always been the focus of tire research (Nakajima *et al*., 1996). In order to investigate the tire's structural mechanism, lots of models have been put forward. The earliest research about theory of carcass contour was the tire cross-section contour theory put forward by Purdy (1963), then Robecchi proposed the mesh model of tire (Robecchi and Amici, 1973), and Hofferberth proposed a cross-section contour design theory of bias tire which was used to study cord's reinforcement effect on rubber and tire's deformation under load adopting couple-stress theory (Hofferberth, 1956). However, these theories cannot accurately reflect the actual structure characteristics of tire because the mesh theory and thin film theory ignore the influence of the rubber around the cord on the carcass contour (Lee *et al*., 2011). The unique structure of the belt in radial tires reduces the load capacity of the crown's carcass layer (Ogawa *et al*., 1990). Therefore, the traditional contour theories of bias tire are no longer suitable to the structure design of radial tires.

In order to take the pressure share effect of the belt into consideration, Japanese scholar Sakai put forward the concept of pressure share ratio (Sakai, 1987). It directly defined the pressure share ratio function of the crown and lower sidewall, and considered that the distribution shape of pressure share ratio is a downwards parabola in the crown, but a straight line in the lower sidewall. Then the distribution law of belt pressure share ratio gradually became the focus of tire research. Böhm and Frank published the research results about the cross-section shape of radial tires, which indicated that the belt pressure share ratio is more consistent with the law of uniform distribution (Böhm, 1965). On the assumption that the belt pressure share ratio is constant across the width of the belt, the tire cross-section contour curve integral equation was derived. Akasaka combined the tire equilibrium contour theories with the non-equilibrium contour theories and got a new grand unified theory of tire, which is GUTT theory (Akasaka *et al*., 1990).

Among the numerous design parameters that affect the carcass contours, the influence of the pressure share ratio is more distinct than other parameters. However, problems regarding how to determine the belt pressure share ratio and the rationality of the distribution function of pressure share ratio remain unresolved, and few studies consider the impact of belt pressure share ratio on the carcass contour and tire performance.

Based on the new non-natural equilibrium contour theory proposed by author's group (Yang *et al*., 2016), this paper selected the 385/65R22.5 all-steel radial tire as the research object, and used finite element analysis to study the effect of belt pressure share ratio on the carcass contour and tire

**Corresponding author*. e-mail: yangjian@ujs.edu.cn

performance. The tire carcass contours, tire wear, footprint, rolling resistance and grip performance have been studied under different belt pressure share ratios.

2. FINITE ELEMENT ANALYSIS OF BELT PRESSURE SHARE RATIO

2.1. Finite Element Model

The contact pressure between the belt layer and carcass surface generally represents the sharing degree of the belt layer for the inflation pressure, which is pressure share ratio of the belt layer, and it can be defined by the following equation:

$$\xi = \frac{\sigma_n}{P} \tag{1}$$

Where, σ_n means the radial contact stress between the belt layer and carcass layer; p means the inflation pressure.

The belt layer and carcass layer were modeled separately using ABAQUS software, and assuming no sliding contact at the interface, which is put forward by Li (2003). During the simulation of two-dimensional tire inflation, the contact pressure between the belt layer and carcass layer can be obtained, and then the pressure share ratio of the belt layer can be calculated using the equation above.

Considering the influence of the tire type and structural parameters on the belt pressure share ratio, this paper selected 11.00R20, 315/60R22.5 and 385/65R22.5 tires for analysis and comparison. The more common '4-layers' and '3 + 0°' belts structures are used in the analysis. The modeling process is shown in Figure 1.

When utilizing ABAQUS for finite element analysis, the Yeoh and Rebar models are used to characterize the material properties of rubber element and steel cord element, respectively (Sorenson, 2003). In this model, tire rim is simplified as an analytical rigid body, adopting interference fit between the bead, and the contact surface between the carcass layer and the belt layer using the Tie constraint mode. The two-dimensional finite element models of 11.00R20, 315/60R22.5 and 385/65R22.5 tires are shown in Figure 2.

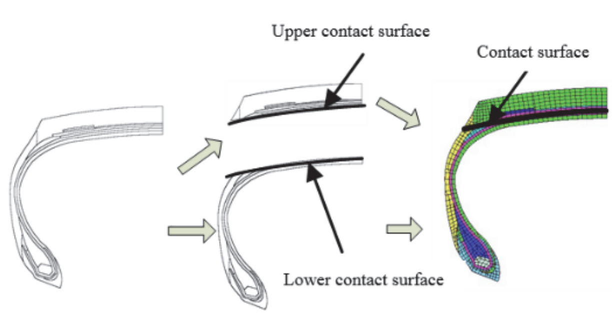

Figure 1. Modeling process.

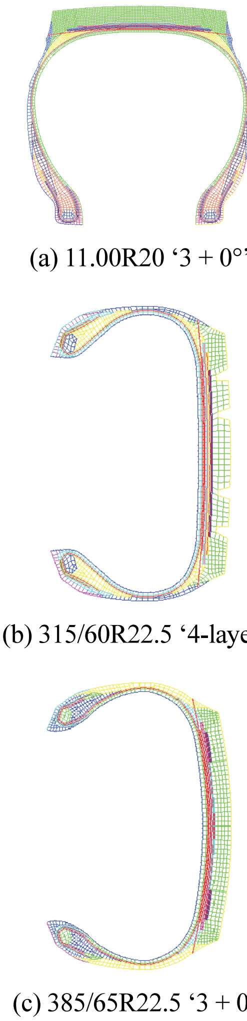

Figure 2. 2D finite element model of tire.

2.2. Results of Finite Element Analysis

The normal contact stress between the belt layer and the carcass layer can be obtained by inflation analysis using ABAQUS software. The belt pressure share ratio can be calculated according to the Equation (1), as shown in Figure 3.

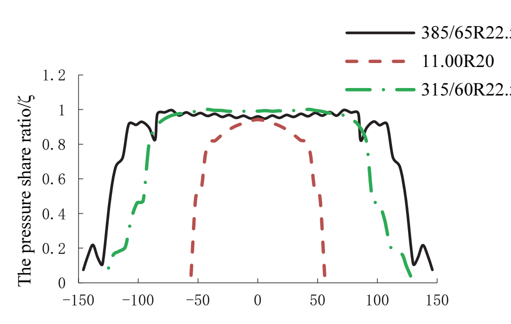

Figure 3. Belt layer pressure share ratio.

It can be seen from Figure 3, for the 315/60R22.5 and 385/65R22.5 tires with a lower flat ratio, the shape of the distribution of the belt pressure share ratio is almost equal to the trapezoid within the width range of belt layer, and the distribution of the belt pressure share ratio of two tires is similar. The fluctuations in the middle part of the belt layer are very small and almost remain constant, while the pressure share ratio shows a slight decline on both sides because the curvature of the carcass in this part has a more significant change than in the middle part, the shoulder wedge added between the belt layer and carcass layer makes them no longer fit tightly. At the ends of the belt layer, the belt pressure share ratio drops sharply. For the 11.00R20 tire, the belt pressure share ratio is parabolically distributed in the width of the belt layer, and decreases approximately vertically at both ends.

It can be inferred that, for conventional tires, the pressure share ratio of the belt layer is approximately parabolic within its width range due to the narrow section width, which leads to a larger crown expansion during inflation. For wide-base tires, the pressure share ratio of the belt layer is approximately constant over its width.

3. NEW NON-NATURAL EQUILIBRIUM CONTOUR THEORY

Böhm and Frank analyzed the section shape of radial tire based on the network theory. Frank believed that the distribution of pressure share ratio g between carcass and belt layer was closer to a trapezoidal curve than a parabola, and the pressure share ratio could be considered as a constant within the width of the belt layer. Thereafter, Sakai Hideo put forward that the internal pressure of the tire was not entirely borne by the carcass layer, on the contrary, the belt layer and the strength layer bear most pressure.

Considering Frank and Sakai Hideo's viewpoints, Frank's formula was applied to the part of crown, while Sakai Hideo's formula was applied to the middle part of sidewall and the lower sidewall, Yang *et al.* (2016) proposed a new non-natural equilibrium contour design theory. To achieve the calculation of cross-section contour curve for the radial tire with belt layer and strength layer, the section contour should be divided into three parts, as shown in Figure 4. The respective contour parts are calculated as follows.

(1) Belt layer parts of crown (K-D interval shown in Figure 4)

$$y_d = y_m - \int_{r_m}^{r_d} G_2(r)dr$$

$$y = y_d - \int_{r_d}^{r} [(r_d^2 - r_m^2) + \zeta(r^2 - r_d^2)]\, dr \,/ \{[(r_d^2 - r_m^2) + \zeta(r_k^2 - r_d^2)]^2 - [(r_d^2 - r_m^2) + \zeta(r^2 - r_d^2)]^2\}^{1/2} \quad (2)$$

Where,

$$G_2(r) = (r^2 - r_m^2)[B^2 - (r^2 - r_m^2)^2]^{-1/2}$$

$$B = r_d^2 - r_m^2 + (1 - \tau_0 + \frac{a r_k}{r_k - r_d})(r_k^2 - r_d^2) - \frac{2a(r_k^3 - r_d^3)}{3(r_k - r_d)}$$

Where $\zeta = 1 - g$, g means the pressure share ratio, r_k is the radius of the crown to the rotation axis, r_d is the radius of the belt to the rotation axis, τ_0 is the belt pressure share ratio, r_m is the section radius at the maximum width, y_m is the width of the tire.

(2) Middle sidewall (D-E interval shown in Figure 4)

$$y = \int_{r_d}^{r_k} G_1(r)\mathrm{d}r + \int_{r}^{r_d} G_2(r)\mathrm{d}r \quad (3)$$

Where,

$$G_1(r) = [r_d^2 - r_m^2 + (1 - \tau_0 + \frac{a r_k}{r_k - r_d})(r^2 - r_d^2) - \frac{2a(r^3 - r_d^3)}{3(r_k - r_d)}] \times \{B^2 - [r_d^2 - r_m^2 + (1 - \tau_0 + \frac{a r_k}{r_k - r_d})(r^2 - r_d^2) - \frac{2a(r^3 - r_d^3)}{3(r_k - r_d)}]^2\}^{-1/2}$$

(3) Strength layer parts (E-B interval shown in Figure 4)

$$y = \int_{r_d}^{r_k} G_1(r)\mathrm{d}r + \int_{r_e}^{r_d} G_2(r)\mathrm{d}r + \int_{r}^{r_e} G_3(r)\mathrm{d}r \quad (4)$$

Where,

$$G_3(r) = [r_e^2 - r_m^2 + (1 - \frac{\tau_e r_e}{r_e - r_b})(r^2 - r_e^2) + \frac{2\tau_e(r^3 - r_e^3)}{3(r_e - r_b)}] \times \{B^2 - [r_e^2 - r_m^2 + (1 - \frac{\tau_e r_e}{r_e - r_b})(r^2 - r_e^2) + \frac{2\tau_e(r^3 - r_e^3)}{3(r_e - r_b)}]^2\}^{-1/2}$$

Where, r_e means the radius of strength to the rotation axis, r_b is the radius of bead center to the rotation axis and τ_e is the strength pressure share ratio.

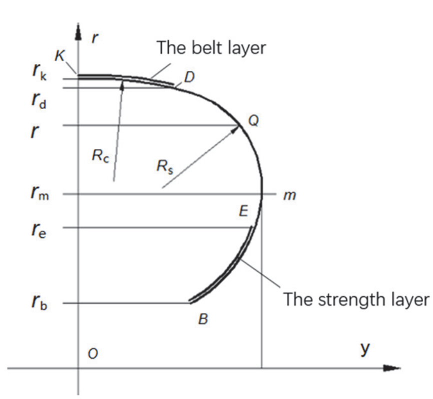

Figure 4. Radial tire contour with belt layer and strength layer.

According to the Equations (2) ~ (4), the tire section contour curves can be obtained.

4. INFLUENCE OF BELT PRESSURE SHARE RATIO ON CARCASS CONTOUR AND TIRE PERFORMANCE

4.1. Influence of Belt Pressure Share Ratio on Carcass Contour

Tires produced by tire manufacturers must conform to pneumatic tire design standards and manuals (Pan, 2011). Taking 385/65R22.5 all-steel radial tire as the research object and belt pressure share ratio as design variable, this paper explores the influence law of belt layer pressure share ratio on carcass contour based on the new non-natural equilibrium contour design theory for radial tire. Under the condition that the width of tire section has been determined, in order to compare the influence law of different belt layer pressure share ratios on the carcass contour, referring to the research of Pan (Yu and Ding, 2006), four different belt pressure distribution ratios were selected for comparison in this paper. Design parameters are shown in Table 1.

According to the design parameters of Table 1, the carcass contour curves of different belt layer pressure sharing rates can be designed by using the contour design software, which can be seen in Figure 5.

It can be seen from Figure 5, the curvature of the crown increases, and the shape becomes more rounded as the belt-pressure share ratio increases. Because the belt layer and the carcass layer fit tightly against each other at the mid-crown area, the radius of curvature of them is basically identical. The curve of carcass layer contour at crown area tends to be rounded with the increase of belt pressure share ratio. From the above analysis, the increase of the belt layer pressure share ratio means that the wrapping effect of the belt layer is enhanced. From the point of tire structure design, the increase of belt pressure share ratio leads to the rounded tendency of tire section contour, and this provides a design suggestion for changing the pressure share ratio of the belt layer.

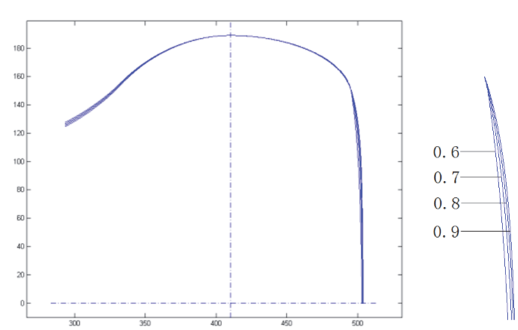

Figure 5. Carcass contours of different belt pressure share ratio (mm).

4.2. Influence of Belt Pressure Share Ratio on Tire Performances

According to the analysis above, the change in the belt pressure share ratio results in a change in the carcass contour, which in turn impacts the tire performance. However, the effect law of belt pressure share ratio on tire performance is not clear so far. For the purpose of providing guidance for engineers to design specific performance tires, we studied the changing laws of tire wear, footprint, rolling resistance and grip performance under different belt pressure share ratios. For 385/65R22.5 tire we selected, the width of the tire chafer area is generally determined by the size of rim. The above results show that the change of the belt layer pressure share ratio only affects the shape of crown and has little effect on the shape of lower sidewall, which is one of the most concerning problems for tire engineers (Fang, 2007). Considering the practical feasibility, the tire structure designed according to 4 different belt pressure share ratios is shown in Figure 6.

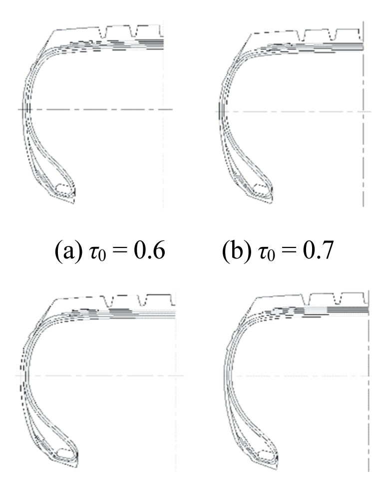

(a) $\tau_0 = 0.6$ (b) $\tau_0 = 0.7$ (c) $\tau_0 = 0.8$ (d) $\tau_0 = 0.9$

Figure 6. Tire structure with different belt pressure share ratio.

Table 1. Parameters under different belt pressure share ratios.

Tire type	Design parameters											
	y_m/mm	r_k/mm	r_d/mm	r_m/mm	r_e/mm	r_b/mm	τ_{01}	τ_{02}	τ_{03}	τ_{04}	τ_e	a
385/65R22.5	189.0	504.1	495.8	410.0	332.8	293.5	0.9	0.8	0.7	0.6	0.11	0.10

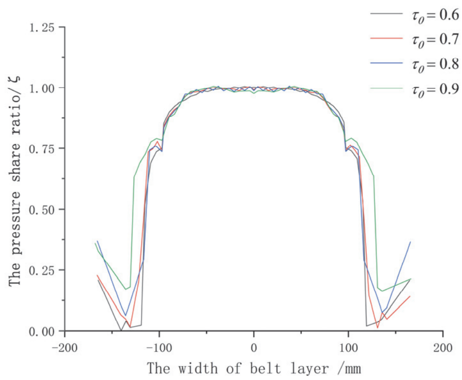

Figure 7. Distribution of belt layer pressure share ratio.

Based on the tire structure in Figure 6, the belt pressure share ratio of the tire under different design variables was calculated, as shown in Figure 7.

It can be seen from Figure 7, the pressure share ratio is a constant value in the middle of the belt and declines sharply at both ends. With the increase of the design variable, the pressure sharing rate at both ends also increases. It can be deduced that when the design factors grow, the belt curve flattens, resulting in a rise in the belt pressure share ratio at both ends.

4.3. Influence of Belt Pressure Share Ratio on Tire Wear Performance

4.3.1. Finite element model

The rubber material is defined by CGAX3H and CGAX4H elements, and the steel cord is defined by Rebar layer when building the finite element analysis model of tire (Liang, 2013). The 2D finite element analysis model is established according to the structure of tire that is shown in Figure 6, which consists of 1664 elements and 1843 nodes in total, as shown in Figure 8. In the 3D finite element model shown in Figure 9, the total number of cells is 199680 and the number of nodes is 221160. Rims and pavements are defined as analytic rigid bodies, and the friction between the pavement and the tread, bead and the rim should be considered. The accuracy of the finite model has been confirmed by Fang and Lu (2002).

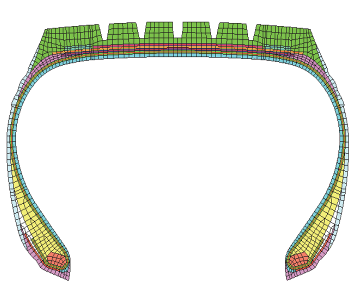

Figure 8. 2D finite element model.

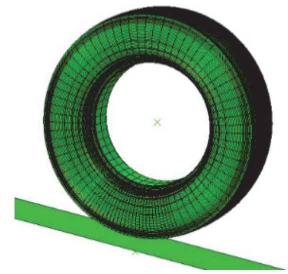

Figure 9. 3D finite element model.

4.3.2. Finite element simulation of tire wear

It is generally assumed that tread wear is caused by friction loss, and the wear amount is proportional to the exponent of the frictional energy of the contact area between tire and pavement. Therefore, the frictional energy of the contact area is used to evaluate tire wear performance in this paper.

4.3.2.1. Calculation method of tire frictional energy

Energy loss is inevitable in the process of rolling contact between tire and ground. Considering the effect of friction and tire deformation, the frictional energy loss is the following equation (He *et al*., 2010).

$$E = \int \vec{F_s} \cdot d\vec{S} \tag{10}$$

Where, F_s means the shear force in contact patch area; s means the displacement of the tread point in contact patch area.

4.3.2.2. Boundary condition setting

The boundary condition is set as shown in Table 2, where the slip rate is selected by referencing the literature (Wang and Wu, 2011).

4.3.2.3. Simulation results

According to the tire finite element model of Figure 6, ABAQUS is used to simulate the friction energy loss on the

Table 2. Tire wearing boundary conditions.

Type	Boundary conditions				
	Pressure (Pa)	Load (kg)	Friction coefficient	Velocity ($m \cdot s^{-1}$)	Slip rate
385/65R22.5	830,000	4,250	0.7	22.2	0.02

Table 3. Frictional energy loss.

Type	385/65R22.5HN207			
	$\tau_0 = 0.6$	$\tau_0 = 0.7$	$\tau_0 = 0.8$	$\tau_0 = 0.9$
Friction energy (J)	548.7	558.8	570.4	583.2

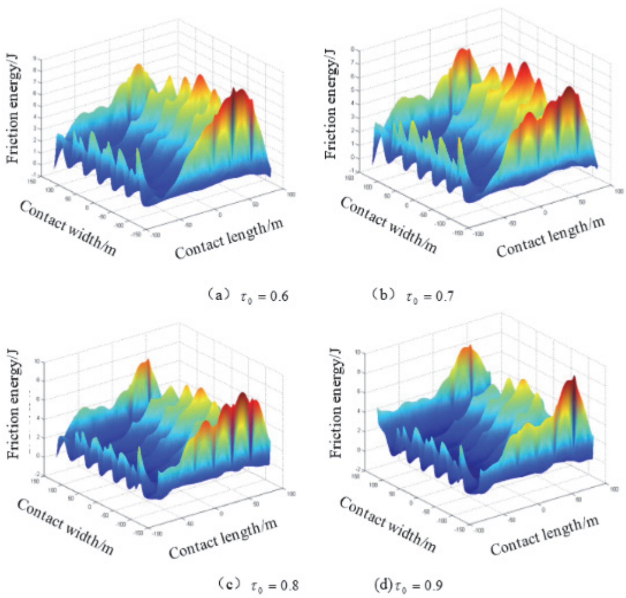

Figure 10. Distribution of frictional energy for free rolling tire.

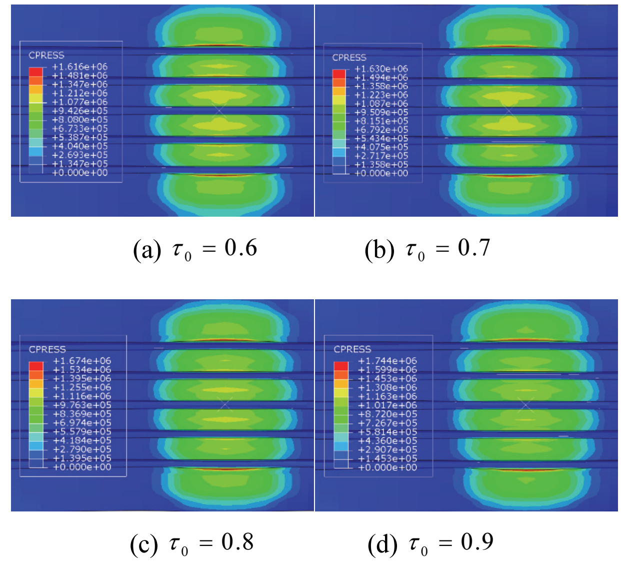

Figure 11. Tire footprint shape and contact pressure distribution (Pa).

contact surface under the free rolling state of tire. The simulation results of tire wear performances under different belt pressure share ratios are shown in Table 3.

It can be seen from Table 3 that the frictional energy between tire tread and ground increases with the increase of the belt layer pressure share ratio. Further analysis indicates that the increased amplification of frictional energy of the contact area is basically equal, only shows slightly increase with the belt layer pressure share ratio increases. As it can be seen from Figure 10, the frictional energy is mainly concentrated on the front and rear ends of contact patch while it is basically zero in the center. The frictional energy at the front end of the rolling direction is much larger than the rear end. This is mainly due to the tire footprint center being slightly forward during tire free rolling state. As the rubber of the front end of the contact patch is squeezed, the slip amount generated by the front end of the rolling direction is larger than the other area. With the increase of the belt pressure share ratio, the concentration phenomenon of the tire shoulder's frictional energy is enhanced, uneven wear increases, and the frictional energy loss increases.

4.4. Influence of Belt Pressure Share Ratio on Tire Footprint

The tire footprint shape and contact pressure distribution under static loading are analyzed. According to the finite element model in Figure 6, tire footprint is simulated by ABAQUS with 830,000 Pa of inflation pressure and 35,426 N of the static loading pressure. The comparison results of different belt pressure share ratios are shown in Figure 11.

As shown in Figure 11, the footprints of the 385/65R22.5 tires under different belt pressure share ratios are similar in shape and roughly distributed in a rectangle. There is a local stress concentration phenomenon in the grooves on both sides of the tire, and as the belt pressure share ratio increases, the concentrated stress in the grooves increases. It can be inferred that the curvature of the crown increases as belt pressure share ratio increases, intensifying the stress concentration phenomenon at the tire shoulder.

4.5. Influence of Belt Pressure Share Ratio on Tire Rolling Resistance

According to the finite element model in Figure 6, tire rolling resistance at the speed of 22.2 m/s is simulated by ABAQUS. Then a method proposed by Wang was used to analyze the influence of different belt layer pressure share ratios on tire rolling resistance (Wang and Wu, 2011). The simulation results are shown in Table 4.

It can be seen from Table 4 that there is a nonlinear negative correlation between the belt pressure share ratio and tire rolling resistance, which is shown in Figure 12. As it is described in Figure 12, the belt layer pressure share ratio increases while the tire rolling resistance decreases. Further analysis shows that the rolling resistance decreases slightly with the increase of the belt layer pressure share ratio when $\tau_0 > 0.7$. The rolling resistance increases obviously with the reduction of the belt pressure share ratio when $\tau_0 < 0.7$. Therefore, this conclusion can be drawn, the flat crown design is beneficial to reduce the rolling resistance.

Table 4. Tire rolling resistance under free rolling.

Type	385/65R22.5HN207			
	$\tau_0 = 0.6$	$\tau_0 = 0.7$	$\tau_0 = 0.8$	$\tau_0 = 0.9$
Rolling resistance (N)	177	170	168	167

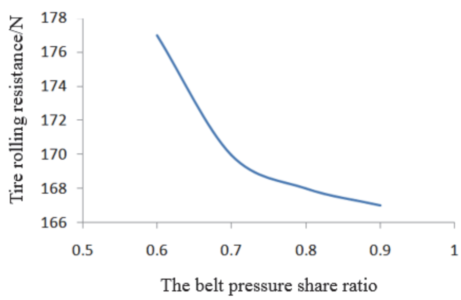

Figure 12. Trend of the tire rolling resistance.

Table 5. Maximum of tangential force in braking.

Type	385/65R22.5			
	$\tau_0 = 0.6$	$\tau_0 = 0.7$	$\tau_0 = 0.8$	$\tau_0 = 0.9$
Maximum braking force (N)	24264	24273	24283	24290

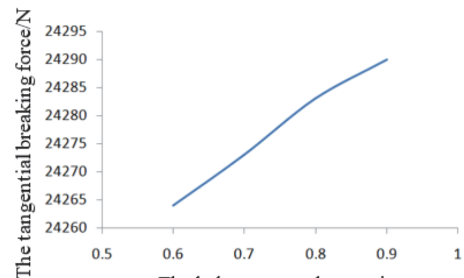

Figure 13. Trend of tangential breaking force.

4.6. Influence of Belt Pressure Share Ratio on Grip Performance of Tire

The influence of different belt pressure share ratios on tire grip performance is analyzed. According to the finite element model of Figure 6, the braking state of tire at the speed of 22.2 m/s is also simulated by ABAQUS. The maximum tangential force between the tire and ground is obtained to evaluate tire grip performance. The simulation results are shown in Table 5.

It can be seen that there is a linear positive correlation between the belt pressure sharing rate and the tire's grip performance, as shown in Figure 13. And as the belt pressure sharing rate increases, the tire grip performance is gradually increased, but the amplitude is not obvious. Combining the results of the friction energy loss in Table 3, there is a contradiction between the grip and wear performances of the tire. From the view of contact pressure distribution during braking process (Figure 14), the contact shape changes, the center of the footprint moves to the rear of the brake state, and the stress concentration occurs in the tire shoulder area. The shoulder contact pressure concentration is increased as the belt layer pressure share ratio increases. Therefore, to a certain extent, the stress concentration of tire shoulder is good for improving tire grip performance. It can be inferred that, under the premise of ensuring the overall uniform distribution of contact pressure, making the contact pressure concentration on the tire shoulder by the design of tread local area is beneficial to enhance the grip performance.

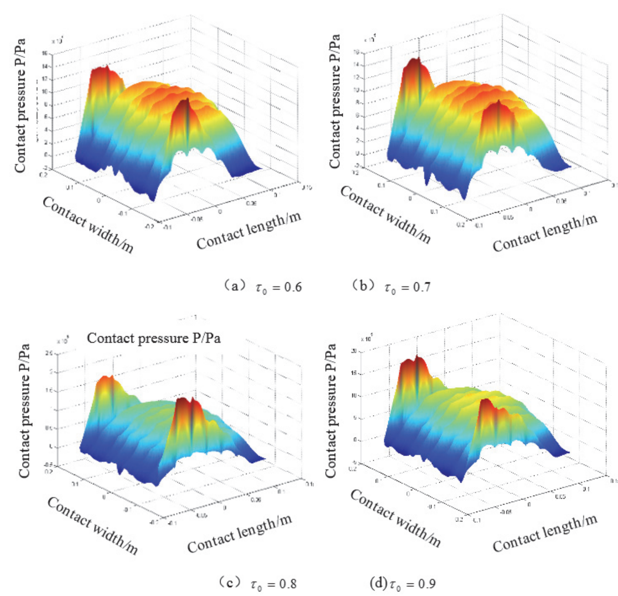

Figure 14. Distribution of contact pressure under tire full brake state.

5. CONCLUSION

Based on the new non-natural equilibrium contour design theory, and taking 385/65R22.5 as the research object, this paper explores the influence law of the tire design parameters on the carcass contours and the tire performance. The conclusions are drawn as follows:

(1) For wide-base tires, within the belt layer width range, the belt pressure share ratio is almost a trapezoidal distribution. The fluctuations in the middle part of the belt layer are very small and can be regarded as constant, while the pressure share ratio shows a slight decline at both ends and abruptly decreases at the end of belt layer.

(2) With the increase of the pressure share ratio of belt layer, the wrapping effect of the belt layer on carcass is enhanced, curvature of carcass contour in the crown part increases, crown curve tends to be rounded.
(3) The belt pressure share ratio has a significant effect on tire performance. According to the research, with the increase of the pressure share ratio, tire wear and grip performances are enhanced while tire rolling resistance performance reduced.

ACKNOWLEDGEMENT–This work is supported by National Natural Science Foundation of China (51405201). The authors would like to express their gratitude to Mr. Wan Zhijun from YFKSS for his invaluable help in compiling the MATLAB program. Mr. Li Zhao from AEOLUS TYRE CO., LTD. also provides lots of help in tire contour design.

REFERENCES

Akasaka, T., Katoh, M., Nihei, S. and Hiraiwa, M. (1990). Two-Dimensional Contact Pressure Distribution of a Radial Tire. *Tire Science and Technology* **18**, **2**, 80–103.

Böhm, F. (1965). Zur Mechanik von Luftreifen. *ZAMM-J. Applied Mathematics and Mechanics/ Zeitschrift für Angewandte Mathematik und Mechanik* **45**, **S1**, T104–T105.

Fang, C. (2007). *Nonlinear Finite Element Analysis for Radial Heavy Duty Tire Based on Rebar Element*. Ph. D. Dissertation. Jiangsu University. Zhenjiang, China.

Fang, Q. H., Lu, J. L., Zhao, L. Q. and Li X. R. (2002). Study on model for energy dissipation in finite element analysis of tire wear. *Journal of Shenyang Institute of Chemical Technolgy* **16**, **3**, 228−231.

Frank, F. and Hofferberth, W. (1967). Mechanics of the Pneumatic Tire. *Rubber Chemistry and Technology* **40**, **1**, 271–322.

He, T., Li, Z. R. and Wang, Y. (2010). Finite element analysis for sliding abrasion of tread blocks of radial tire. *Engineering Mechanics* **27**, **7**, 237−243.

Lee, D. W., Kim, J. K., Kim, S. R. and Lee, K. H. (2011). Shape design of a tire contour based on approximation model. *J. Mechanical Science and Technology* **25**, **1**, 149–155.

Li, W. (2003). *Radial Tires Finite Element Structural Analysis and Some Basic Problems in Design Principles.* Ph. D. Dissertation. University of Science and Technology of China. Hefei, China.

Liang, C. (2013). *Research on Radial Tire Comprehensive Ground Performance Evaluation System and Method*. Ph. D. Dissertation. Jiangsu University. Zhenjiang, China.

Nakajima, Y., Kamegawa, T. and Abe, A. (1996). Theory of optimum tire contour and its application. *Tire Science and Technology* **24**, **3**, 184–203.

Ogawa, H., Furuya, S., Koseki, H., Iida, H., Sato, K. and Yamagishi, K. (1990). A study on the contour of the truck and bus radial tire. *Tire Science and Technology* **18**, **4**, 236–261.

Pan, T. (2011). *Some Theory Study of Contour Design for Radial Tire*. Ph. D. Dissertation. South China University of Technology. Guangzhou, China.

Purdy, J. F. (1963). *Mathematics Underlying Design of Pneumatic Tires*. 1st edn. Edwards Brothers. Ann Arbor, Michigan, USA.

Robecchi, E. and Amici, L. (1973). Mechanics of the pneumatic tire. Part I. The tire under inflation alone. *Tire Science and Technology* **1**, **3**, 290–345.

Sakai, H. (1987). *Tire Engineering*. 2nd edn. Grand Prix of Corporation Publication. Tokyo, Japan.

Sorenson, H. K. (2003). ABAQUS Version 6.4: Theory Manual, Users' Manual. *Hibbitt*, *Karlson*, *Sorenson Inc*. USA.

Wang, G. L. and Wu, J. J. (2011). Finite element analysis of truck radial tire rolling resistance. *Computer Simulation* **27**, **11**, 332–334.

Yang, J., Wang, G. L., Wan, Z. J., Liang, C. and Zhou, H. C. (2016). Non-natural equilibrium contour design for radial tire and its influence on tire performance. *Int. J. Automotive Technology* **17**, **4**, 639–649.

Yu, Q. and Ding, J. P. (2006). *Radial Tire Structure Design and Manufacturing Technology*. 2nd edn. Chemical Industry Press. Beijing, China.